Reac Kinet Mech Cat (2016) 117:583–591
DOI 10.1007/s11144-015-0948-7

Catalytic activity of MnO_x/TiO_2 catalysts synthesized with different manganese precursors for the selective catalytic reduction of nitrogen oxides

Sungchul Hwang[1] · Seung-Hyeon Jo[2] · Janghoon Kim[3] · Min-Chul Shin[4] · Ho Hwan Chun[5] · Hyun Park[6] · Heesoo Lee[2]

Received: 6 August 2015 / Accepted: 1 November 2015 / Published online: 14 November 2015

Abstract The effects of different manganese precursors on the low-temperature (100–300 °C) selective catalytic reduction of nitrogen oxide (NO_x) were investigated. MnO_x/TiO_2 catalysts were prepared by a sol–gel method using three different precursors, manganese(II) nitrate (MN), manganese(II) acetate (MA2), and manganese(III) acetate (MA3). They had an overall high specific surface area, but the relatively small surface areas of MN–MnO_x/TiO_2 and MA3–MnO_x/TiO_2 were due to the existence of a Mn_3O_4 phase in these catalysts. There is no chemical reaction at the working temperature, which proves the high thermal stability of all the catalysts. The result of de-NO_x (removal of NO_x) efficiency in the low temperature region showed that the catalyst synthesized with manganese acetate had higher catalytic activity than the catalyst synthesized with manganese nitrate. Despite the relatively small surface area, the MA3–MnO_x/TiO_2 exhibited the highest de-NO_x efficiency, which resulted from the most enriched Mn concentration and Mn^{4+} species (MnO_2) as well as strong acid sites on catalyst surface.

✉ Heesoo Lee
heesoo@pusan.ac.kr

[1] Graduate School of Convergence Science, Pusan National University, Busan 609-735, Korea

[2] School of Materials Science and Engineering, Pusan National University, Busan 609-735, Korea

[3] Technical Research Laboratories Pohang Research Lab, POSCO, Pohang 790-300, Korea

[4] Material Technology Center, Korea Testing Laboratory, Seoul 152-718, Korea

[5] Department of Naval Architecture & Ocean Engineering, Pusan National University, Busan 609-735, Korea

[6] Global Core Research Center for Ships and Offshore Plants, Pusan National University, Busan 609-735, Korea

Keywords MnO_x/TiO_2 · Manganese precursor · de-NO_x efficiency · Surface valence state

Introduction

The selective catalytic reduction (SCR) of NO_x with NH_3 is an effective technique for removing NO_x from flue gases of stationary sources [1, 2]. The commercial catalyst, V_2O_5/TiO_2 (anatase) with either WO_3 or MoO_3, has high activity and stability for the use in SCR of NO_x with NH_3 at 300–400 °C [3–5]. However, SO_2 and the high concentrations of ash in the flue gas reduce their performance and durability because this type of catalyst is always placed before dust precipitation and flue gas desulphurization system [6, 7]. Therefore, the trend is to develop low-temperature catalysts capable of working at the end of the exhaust system without the reheating [8].

In the low temperature SCR, the commercial catalyst cannot be defined. Most of the investigated catalysts were noble metal and transition metal oxides (Cr, Mn, Fe, Co, Ni, and Cu). The research of noble metal catalyst was focused on the catalyst support such as SiO_2, Al_2O_3 [9], mesoporous silica [10], zeolites [11], TiO_2–ZrO_2 [12], and MgO–CeO_2 [13]. It was reported that 50 and 75 % NO conversions were obtained over Pt/Al_2O_3 catalyst at 140 °C and over Pt/SiO_2 catalyst at 90 °C [14]. A large number of catalysts consisted of various transition metal (Cr, Mn, Fe, Co, Ni, and Cu) oxides on different commercial supports have been investigated for low temperature SCR reactions, which can be capable of operating in the temperature range 100–300 °C. Among all the zeolite-based catalysts, Fe-ZSM-5 and Cu-ZSM-5 have been the most extensively investigated in the past 20 years. At temperatures over 350 °C on 2.5 % Fe/ZSM-5, the NO conversion reached nearly 90 % and also with a wide temperature window [15, 16]. Manganese oxides supported on TiO_2 have relatively high activity for low temperature SCR of NO_x with NH_3 among these catalysts [17]. Manganese oxide was the main catalyst (active phase) and titanium oxide was the catalyst support in this composite. The active phase acts as a decomposition catalyst of the nitrogen oxide (NO_x) to nitrogen and water. The catalyst support formed a large surface area and ensured that the shape of the active phase was maintained. Titanium oxide does not have activity in the SCR reaction [18]. It has been documented that MnO_x–Al_2O_3 prepared using the manganese acetate (MA) precursor shows better dispersion of MnO_x on alumina and higher catalytic activity than manganese nitrate (MN) at 100-180 °C [19]. It has also been reported that the MnO_x/TiO_2 catalyst prepared from MN resulted in a better performance than that prepared from the MA precursor at 100–200 °C [20].

In this study, commonly used precursors [manganese(II) acetate, manganese(III) acetate, and manganese(II) nitrate] were chosen for the synthesis of MnO_x/TiO_2 catalysts but the manganese(III) nitrate was excluded from the comparison because manganese(III) nitrate is an unstable compound, which evolves N_2O_4 at room temperature due to the low thermal stability [21]. The activity of the catalysts synthesized by different precursors were analyzed based on the assumption that the same synthesis condition. Three kinds of the catalyst were characterized by

structural and thermal analysis. The effects of the manganese precursors on the catalytic activity were identified in terms of surface chemical properties.

Experimental

Catalyst preparation

The MnO_x–TiO_2 catalysts were prepared by a sol–gel method with different precursors, manganese(II) nitrate ($Mn(NO_3)_2$, MN), manganese(II) acetate ($Mn(CH_3COO)_2$, MA2), and manganese(III) acetate ($Mn(CH_3COO)_3{\cdot}2H_2O$, MA3). A mixture of titanium(IV) isopropoxide ($Ti[OCH(CH_3)_2]_4$) and ethanol at a 1:10 (by weight) ratio was stirred under reflux at room temperature. A large amount of deionized water and manganese precursors, which are designated as MN, MA2 and MA3, were added and stirred for 24 h. The sol–gel solution was then vaporized at 110 °C until a dry gel was obtained and treated thermally at 400 °C for 2 h. The heating rate was 5 °C/min to promote the decomposition of organic components in the precursor.

Characterization of the catalysts

The specific surface areas of the catalysts were measured by nitrogen adsorption at liquid N_2 temperature (−196 °C), using an ASAP2010 (Micromeritics, USA) adsorption apparatus. Powder X-ray diffraction (XRD) measurements were carried out with a M18XHF (MAC Scientific Co., Netherlands) system with Cu K_α ($\lambda = 0.1543$ nm) radiation. A SDTQ600 (TA Instruments, USA) performed to test the thermal analysis. The samples were heated from room temperature to 700 °C at a rate of 10 °C/min. Fourier transform infrared spectroscopy (FT-IR) monitoring of ammonia adsorption was carried out on a Thermo Nicolet 6700 FT-IR instrument (Thermo Electron Corporation, USA) running at a 4 cm^{-1} resolutions. A gas containing 1000 ppm NH_3 (100 ml/min) was passed through the sample for 1 h at room temperature before the FT-IR experiment. The IR spectra were collected after being purged with N_2 flow gas for 1 h. The atomic surface concentration on each catalyst was analyzed by X-ray photoelectron spectroscopy (XPS, Escalab 250 (Thermo Scientific, UK) using Al K_α (1486.6 eV) as the radiation source. The reference used the $C1_s$ binding energy (BE) of 284.6 eV.

Catalytic activity measurement

The SCR activity was measured in a fixed-bed reactor containing 0.50 ml catalyst at 100–300 °C in 50 °C steps with a gas hourly space velocity of 12,000 h^{-1}. The feed gas mixture consisted of 1000 ppm NO, 1000 ppm NH_3, and 5 % O_2. A total flow rate of 100 ml/min was maintained for all the experiments with N_2 as the balance gas. The flow rate was controlled using a mass flow controller (Sierra Instruments, Inc. and Hi-Tec Co.). The NO and NO_2 concentrations were monitored continually using a NO_x analyzer (42C, Thermo Ins.). An ammonia trap containing a boric acid

solution was installed before the sample inlet to the analyzer to avoid errors due to the oxidation of ammonia in the converter of the NO/NO_x analyzer.

Results and discussion

Fig. 1 shows the XRD patterns of the catalysts prepared from different precursors. The peaks corresponding to the TiO_2 anatase phase were observed on all samples and Mn_3O_4 phase was noted on the MN–MnO_x/TiO_2 and MA3–MnO_x/TiO_2 samples. The manganese oxide phase was not identified at the MA2–MnO_x/TiO_2 sample in the XRD pattern. It was originated from the strong background of TiO_2 and also implies that manganese oxides could have been in a highly dispersed state or manganese ions were inserted into the TiO_2 lattice resulting in the presence of more surface hydroxyl groups in the TiO_2 anatase [22–24]. The surface areas of MN-MnO_x/TiO_2, MA2-MnO_x/TiO_2 and MA3-MnO_x/TiO_2 were 161.32, 174.38, and 155.36 m^2/g. The MN-MnO_x/TiO_2 and MA3-MnO_x/TiO_2 had a small surface area due to the existence of a Mn_3O_4 phase in these catalysts compared to MA2-MnO_x/TiO_2.

Fig. 2 shows the results of thermal analysis on MnO_x/TiO_2. As for MN–MnO_x/TiO_2 and MA2-MnO_x/TiO_2, there are two peaks at around 100 and 680 °C. The peak observed at approximately 100 °C, which was due to the evaporation of water [25]. The sharp peak at around 680 °C can be explained by an anatase to rutile phase transformation. However, the chemical reactions including critical weight loss with exothermic peaks cannot be found at working temperatures. It means that materials were chemically stable at the working temperature. The thermal stability in low temperature SCR was important for long term use and the TG/DSC results proved that all samples was suitable as a low temperature SCR catalyst.

Fig. 3 presents the FT-IR spectra of ammonia adsorbed on MnO_x/TiO_2 catalysts. Two strong peaks at 1667 and 1256 cm^{-1} and a weaker peak at 1460 cm^{-1} were observed. The bands at 1667 and 1460 cm^{-1} were assigned to the symmetric and asymmetric bending vibrations of NH_4^+ chemisorbed on the Brønsted acid sites,

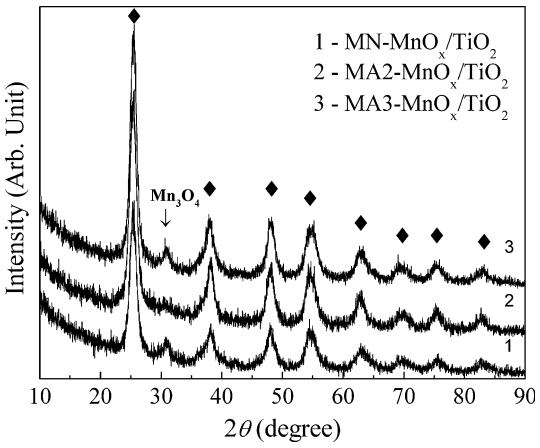

Fig. 1 XRD patterns of TiO_2 and different catalysts powder at room temperature with a Cu Kα ($\lambda = 0.1543$ nm) radiation: *1*—MN-MnO_x/TiO_2; *2*—MA2-MnO_x; *3*—MA3-MnO_x/TiO_2. *filled diamond*—anatase

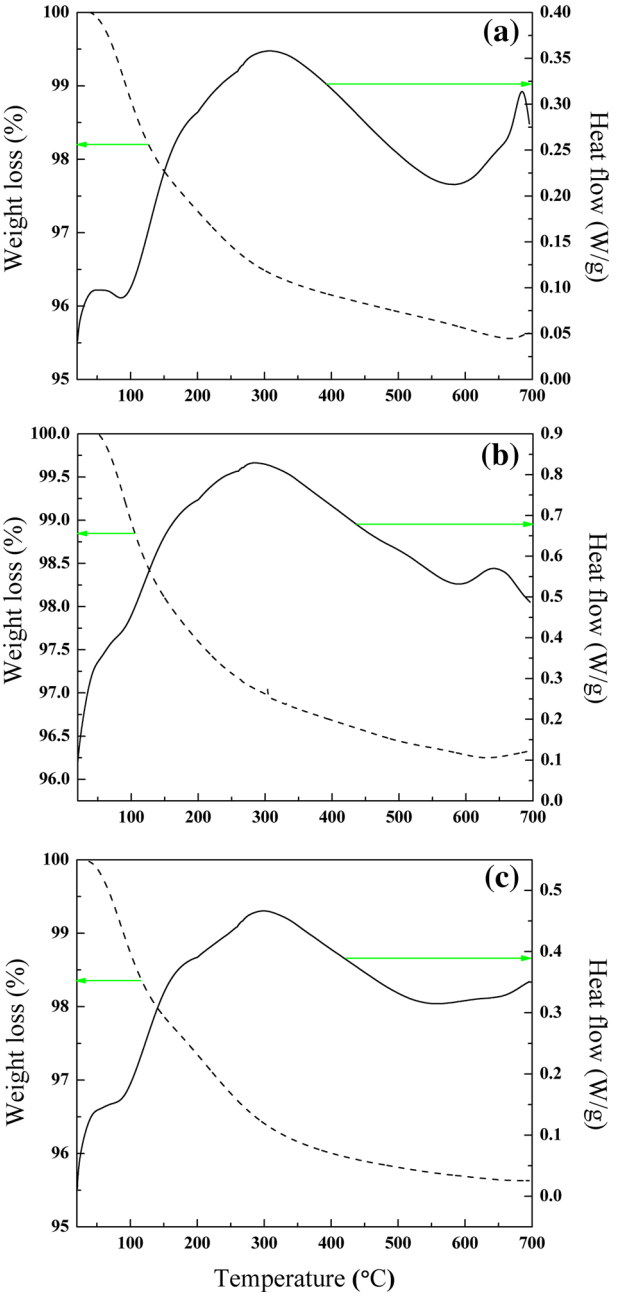

Fig. 2 TG and DTA profiles of different catalysts from room temperature to 700 °C at a rate of 10 °C/min: **a** MN-MnO_x/TiO_2, **b** MA2-MnO_x, **c** MA3-MnO_x/TiO_2

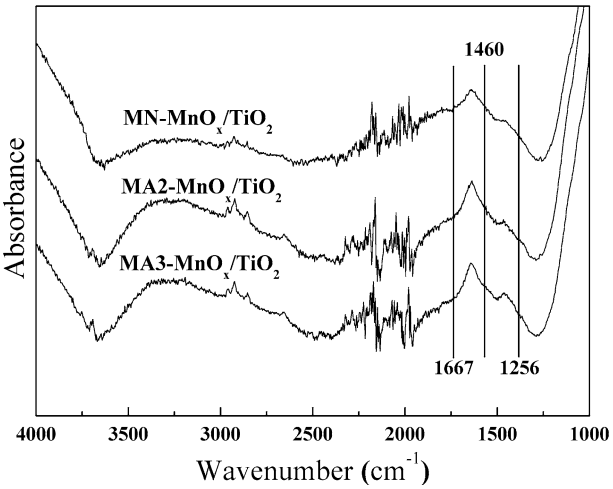

Fig. 3 FT-IR spectra (4 cm^{-1} resolutions) of MnO_x/TiO_2 with different precursor after adsorption of ammonia gas. A gas containing 1000 ppm NH_3 (100 ml/min) was passed through the sample for 1 h at room temperature before the FT-IR experiment

whereas the bands at 1256 cm^{-1} were assigned to vibrations of the N–H bonds in NH_3 linked coordinately to the Lewis acid sites [26–28]. The peak at approximately 1530 cm^{-1} was attributed to amide (NH_2) species. The broad band in the range of 3200–3450 cm^{-1} was assigned to the O–H and N–H stretching vibration, indicating the coordination adsorption of H atom and O atom in metal oxide appear on the catalyst surface [29–31]. For all the peaks, both the peaks of NH_3 adsorption on Brønsted acid sites and Lewis acid sites were obviosuly observed. The MA2-MnO_x/TiO_2 and MA3-MnO_x/TiO_2 catalysts have similar acid sites. The adsorption of ammonia on the MN-MnO_x/TiO_2 catalyst showed relatively weaker acid sites and amide species.

Manganese supported TiO_2 catalysts were examined by XPS to identify the surface atomic concentration and the valence states of Mn interacting with TiO_2 on each catalyst. Fig. 4 shows the Mn 2p photoelectron peaks of the MnO_x/TiO_2 catalysts, and Table 1 lists the relative atomic proportion of Mn and the compositions determined by XPS. Two main peaks due to Mn $2p_{3/2}$ and Mn $2p_{1/2}$ were observed at around 641–653 eV for all samples. The overlapping Mn $2p_{3/2}$ peaks were deconvoluted into several peaks with the use of Shirley type background to identify the surface manganese oxide phases and the results are shown in Table 1. It has been well established that the $2p_{3/2}$ binding energy of the MnO_2 (Mn^{4+}) peak and Mn_2O_3 (Mn^{3+}) peaks appear at 642.1 ± 0.2 and 641.3 ± 0.2 eV, respectively [19, 20, 32]. The SCR of NO over the pure manganese oxides at the low temperature was investigated by Kapteijn et al. [19] and found that the de-NO_x efficiency decreased in the order of $MnO_2 > Mn_5O_8 > Mn_2O_3 > Mn_3O_4$. The MA3-$MnO_x$/$TiO_2$ catalyst had the most enriched Mn concentration and Mn^{4+} species (MnO_2) on the TiO_2 surface. In addition, the MA3-MnO_x/TiO_2 has the highest concentration of Mn on the surface and the Mn/Ti ratio was MA3-MnO_x/TiO_2 > MA2-MnO_x/

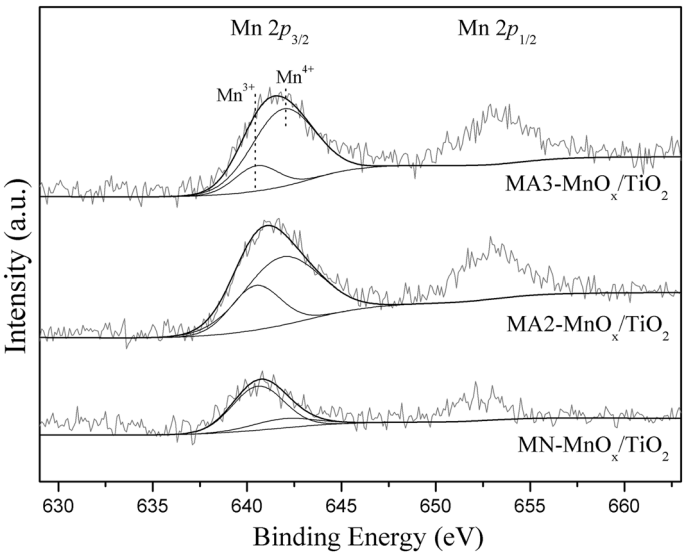

Fig. 4 XPS spectroscopes of different catalysts using AlK_{α} (1486.6 eV) as the radiation source

Table 1 Relative atomic proportion of Mn^{4+}, Mn^{3+}, and compositions of different catalysts

Samples	Mn^{4+}/Mn^{3+} ratio	Proportion (%)		Metal content obtained with XPS (at%)			
		MnO_2	Mn_2O_3	Mn	Ti	O	Mn/Ti
MN-MnO_x/TiO_2	0.25	20.2	79.8	1.8	19.09	53.01	9.42
MA2-MnO_x/TiO_2	2.32	69.9	30.1	2.43	17.95	51.59	13.54
MA3-MnO_x/TiO_2	4.45	81.7	18.3	3.93	18.59	55.56	21.14

TiO_2 > MN-MnO_x/TiO_2. It is well-known that the concentration of Mn on the surface was in the same sequence of the catalytic activity.

The catalytic activity of various manganese precursors on the Mn loaded TiO_2 catalysts were tested for low temperature SCR from 100 to 300 °C. Fig. 5 presents the NO_x conversion results on the above mentioned catalysts. The MnO_x/TiO_2 catalysts showed over 90 % activity at 200 °C, and saturated from this temperature. The MA3-MnO_x/TiO_2 catalyst especially showed higher de-NO_x efficiency than the others in all regions. The difference in atomic concentration or valence states on the surface was considered. The fact that the MA3–MnO_x/TiO_2 showed a relatively higher SCR activity despite showing a lower surface area indicates that the surface area is not significant to the low temperature SCR activity. This is caused by the higher Mn coverage resulting in a higher intensity of NH_3 adsorption and Mn^{4+}/M^{3+} ratio. It is easier to understand why the MA3–MnO_x/TiO_2 catalyst showed better SCR activity because the catalytic reaction is related to the surface MnO_2 and

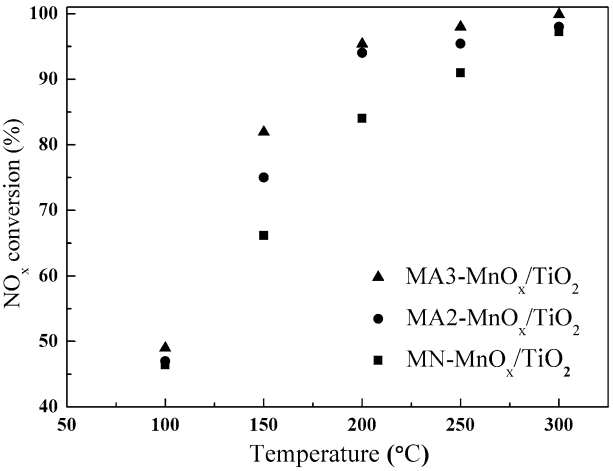

Fig. 5 Catalytic activities of different catalysts for selective reduction of NO with NH_3. Feed: NO and NH_3 = 1000 ppm, O_2 = 5 vol.%, balance N_2; total flow rate = 100 ml/min with 0.50 ml catalyst

NH_2 species [6]. The manganese(III) acetate was the most effective precursor for MnO_x/TiO_2 SCR efficiency for these reasons.

Conclusions

The MnO_x/TiO_2 catalysts were prepared by a sol–gel method using different precursors for the low temperature SCR. The MN-MnO_x/TiO_2 catalyst showed relatively weaker acid sites and amide species than the other samples. The MA2-MnO_x/TiO_2 and MA3-MnO_x/TiO_2 catalysts contained similar acid sites. The catalyst synthesized with manganese acetate had higher catalytic activity than the catalyst synthesized with manganese nitrate. The MA3-MnO_x/TiO_2 catalyst especially showed the highest NO_x conversion under flow conditions of GHSV = 12,000 h^{-1} from 100 to 300 °C with a relatively small specific surface area. The MA3-MnO_x/TiO_2 catalyst was found to be the best for the low temperature SCR of NO with NH_3 among the three different types of precursor catalysts examined. The efficiency of MnO_x/TiO_2 SCR catalyst were able to increase by manganese acetate (III) precursor, because it has enriched Mn concentration and Mn^{4+} species (MnO_2) on the TiO_2 surface.

Acknowledgments This work was supported by the National Research Foundation of Korea (NRF) grant funded by the Korea government (MSIP) through GCRC-SOP (No. 2011-0030013). We are also especially appreciative to Ms. Mary Van Tyne for her language editing of the manuscript.

References

1. Nova I, Ciardelli C, Tronconi E, Chatterjee D, Bandl-Konrad B (2006) Catal Today 114:3–12

2. Gasagrande L, Lietti L, Nova I, Forzatti P, Baiker A (1999) Appl Catal B Environ 22:63–77
3. Bosch H, Janssen F (1988) Catal Today 2:369–379
4. Djerad S, Tifouti L, Crocoll M, Weisweiler W (2004) J Mol Catal A Chem 208:257–265
5. Ettireddy PR, Ettireddy N, Mamedov S, Boolchand P, Smirniotis PG (2007) Appl Catal B Environ 76:123–134
6. Kijlstra WS, Brands DS, Poels EK, Bliek A (1997) J Catal 171:208–218
7. Kijlstra WS, Brands DS, Smit HI, Poels EK, Bliek A (1997) J Catal 171:219–230
8. Tang X, Hao J, Yi H, Li J (2007) Catal Today 126:406–411
9. Yokota K, Fukui M, Tanaka T (1997) Appl Surf Sci 121–122:273–277
10. Wu P, Li L, Yu Q, Wu G, Guan N (2010) Catal Today 158:228–234
11. Shibata J, Hashimoto M, Shimizu K, Yoshida H, Hattori T, Satsuma A (2004) J Phys Chem B 108:18327–18335
12. Machida M, Ikeda S, Kurogi D, Kijima T (2001) Appl Catal B 35:107–116
13. Costa CN, Efstathiou AM (2007) Appl Catal B 72:240–252
14. Burch R, Coleman MD (1999) Appl Catal B 23:115–121
15. Granger P, Parvulescu VI (2011) Chem Rev 111:3155–3207
16. Brandenberger S, Krocher O, Tissler A, Althoff R (2008) Catal Rev 50:492–531
17. Smirniotis PG, PenÄ DA, Uphade BS (2001) Angew Chem Int Ed 40:2479–2482
18. Li P, Xin Y, Li Q, Wang Z, Zhang Z, Zheng L (2012) Environ Sci Technol 46:9600–9605
19. Kapteijn F, Vanlangeveld AD, Moulijn JA, Andreini A, Vuurman MA, Turek AM, Jehng JM, Wachs IE (1994) J Catal 150:94–104
20. Peña DA, Uphade BS, Smirniotis PG (2004) J Catal 221:421–431
21. Johnson DW, Sutton DD (1972) Can J Chem 50:3326–3331
22. Pecchi G, Reyes P, Lopez T, Gomez R, Moreno A, Fierro JLG (2002) J Chem Technol Biotechnol 77:944–949
23. Li J, Chen J, Ke R, Luo C, Hao J (2007) Catal Commun 8:1896–1900
24. Topsoe NY, Topsoe H, Dumesic JA (1994) J Catal 151:226–240
25. Baolong Z (2003) Appl Catal B Environ 40:253–258
26. Kung MC, Kung HH (1985) Catal Rev 27:425–460
27. Belokopytov YV, Kholyavenko KM, Gerei SV (1979) J Catal 60:1–7
28. Topsøe NY (1991) J Catal 128:499–511
29. Liettia L, Ramis G, Berti F, Toledo G, Robba D, Busca G, Forzatti P (1998) Catal Today 42:101–116
30. Matralis H, Ciardelli M, Ruwet M, Grange P (1995) J Catal 157:368–379
31. Zhu J, Gao F, Dong L, Yu W, Qi L, Wang Z, Dong L, Chen Y (2010) Appl Catal B Environ 95:144–152
32. Chen Z, Yang Q, Li H, Li X, Wang L, Chi TS (2010) J Catal 276:56–65